Proceedings of IMECE 2007
2007 International Mechanical Engineering Conference and Exposition
November 11-15, 2007, Seattle, Washington, USA

IMECE2007-44089

THERMAL MEASUREMENT OF HARSH ENVIRONMENTS USING INDIRECT ACOUSTIC PYROMETRY

P.L. Schmidt, D.G. Walker*
Department of Mechanical Engineering
Vanderbilt University
Nashville, TN, 37235

D.E. Yuhas and M.J. Mutton
Industrial Measurement Systems, Inc.
2760 Beverly Drive, Suite 4
Aurora, IL 60502

ABSTRACT

The inversion of a composite governing equation for the estimation of a boundary heat flux from ultrasonic pulse data is presented. The time of flight of the ultrasonic pulse is temperature dependent and can be used to predict the boundary heat flux. Sensitivities of the approach are examined, results from fabricated data are presented, and example solutions are provided with actual ultrasonic temperature measurement data. The results indicate that compared to the canonical inverse heat conduction problem, the additional step of resolving the time-of-flight data to temperature degrades the sensitivities. Nevertheless, sampling the entire temperature distribution enhances the results. This method of using ultrasonic pulses to remotely determine heat fluxes is comparable in terms of accuracy to more common heat flux estimation methods.

INTRODUCTION

Remote sensing of temperature—and perhaps more importantly heat flux—is critical to a number of applications such as wind tunnel measurements, combustion chambers and large gun barrels. Each of these applications involve extremely harsh environments where sensors are not likely to survive or where measurement devices would interfere with the operation of the system. Furthermore, these applications involve high heat fluxes and fast transients. Consequently, high resolution transient characterization of these inaccessible thermal environments is difficult. Using ultrasonic pulses through a conducting wall and inverse methods, the present effort will demonstrate the feasibility of measuring internal heat fluxes in a harsh environment from a remotely mounted sensor.

Ultrasonic pulse measurements have been used in nondestructive evaluation (NDE) for decades with a great deal of success [1]. Furthermore, ultrasonic pyrometry has been used in many process control systems [2] because the sound speed is a strong function of temperature in most materials. This technique has proven effective for gases [3], fluids [4] and extrusions [5] as long as direct access to the material where the temperature is being measured is available. These applications are concerned with average temperature measurements and have not, in general, been used to extract transient heat fluxes.

When a sound wave propagates through a material, its propagation speed will be a function of the local temperature. Therefore the time-of-flight for an ultrasonic pulse will be a function of the temperature distribution along the pulse path [6]. For uniform temperature distributions, the average temperature of the medium can be deduced easily from the time-of-flight calibration data. For non-uniform temperature distributions, the path integral over the unknown temperature must be performed. Although the solution is ill-posed, a priori knowledge of the functional form of the temperature distribution can provide reliable estimates of interior temperatures [7]. Inverse methods have been used to reconstruct steady temperature distributions [8], but transient effects have largely been ignored.

The present analysis will show how ultrasonic temperature measurements can be made on solid structures to extract transient thermal conditions. Transient features are critical to many applications inherent to the aerospace industry. In combustion chambers, for example, internal instabilities need to be characterized

*Address all correspondence to this author.

for effective design of new technologies. However, access to the interior is limited due to the harsh environment and because of possible disruption to the operation of the device. Yet, remote measurement without sacrificing the integrity of the combustion wall is simply not possible with modern measurement systems. Ultrasonic measurement systems allow the sampling of thermal loads in a wall from the presumably benign environment on the outside of the combustion chamber. In order for an ultrasonic measurement system to be viable for accurate characterization of heat fluxes, a technique to recreate the thermal history of time of flight data must be developed. The present work demonstrates this methodology and characterizes the uncertainty in the solution.

A solution approach can be devised from standard inverse techniques. Solutions of the inverse heat conduction problem are predicated on the fact that a discrete number of interior temperatures are known and an unknown boundary condition is wanted. Unlike the traditional inverse heat conduction problem (IHCP), though, the time-of-flight data does not provide local temperatures. Instead, the data represent an integral over the temperature distribution along the pulse path. Consequently, the applicability of traditional methods is uncertain because most solutions are ill-posed in a particular way, and methods are designed to address the instability of particular problems [9]. The present effort will demonstrate the effectiveness of a function specification approach in solving this new class of problems. While actual ultrasonic measurements, where the interior boundary is unknown, are considered, three test cases with manufactured data are examined first. The manufactured data contain similar sample rates, geometry and magnitude of heating as the actual demonstration data. From the test cases, we can evaluate the error introduced by measurement noise and bias inherent to the function specification approach. With the real measured data, external influences will be identified and explained from features in the boundary estimates.

FORMULATION

The inverse solution requires a forward conduction solution to convert an approximate boundary condition to a temperature distribution in the material. Then the temperature distribution is used to predict the time required for an ultrasonic pulse to traverse the medium. The difference between the calculated time of flight and the measured time of flight is minimized by adjusting the approximate boundary condition.

Heat transfer relationships

For the forward conduction solution, consider a one-dimensional solid wall bounded on one surface by a thermally and possibly chemically harsh environment and on the other by ambient conditions. In the present example, the wall is exposed

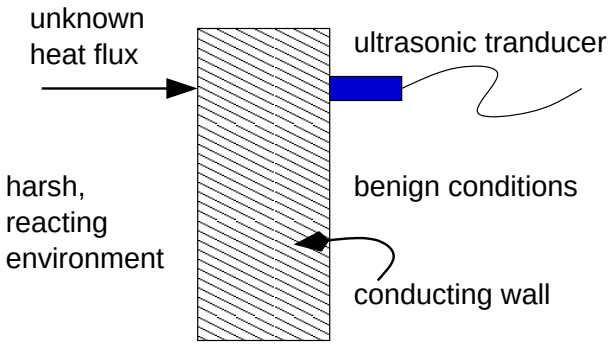

Figure 1. Schematic of the one-dimensional conduction domain where the unknown boundary flux is on the side of the harsh environment and the measurement system (transducer) detects the interior boundary remotely through the wall.

to combustion products whose thermal load is to be measured. The configuration is shown in Figure 1. The governing equation for constant properties is

$$\frac{\partial^2\theta}{\partial x^2} = \frac{1}{\alpha}\frac{\partial\theta}{\partial t}, \quad 0 \le x \le L, \quad t > 0, \tag{1}$$

where x is the position in the wall and θ is the temperature rise above ambient conditions. The internal boundary condition is a time-dependent function for the heat flux

$$-k\frac{\partial\theta}{\partial x} = q(t), \quad x = 0, \quad t > 0, \tag{2}$$

with a specified temperature on the external surface

$$\theta = 0, \quad x = L, \quad t > 0. \tag{3}$$

Here, k is the thermal conductivity of the wall, and L is the thickness of the wall. The initial condition is homogeneous

$$\theta = 0, \quad t = 0, \quad 0 \ge x \ge L. \tag{4}$$

For a constant heat flux at the boundary (independent of time), the temperature solution can be written for constant properties as [10]

$$\theta(x,t) = \frac{2q}{kL}\sum_{m=1}^{\infty}\frac{\cos(\beta_m x)}{\beta_m^2}\exp(-\alpha\beta_m^2 t), \tag{5}$$

where q is constant, α is the thermal diffusivity, and β_m is an eigen-value of the kernel function $\cos(\beta_m x)$, given by

$$\beta_m = \frac{(2m-1)\pi}{2L}. \tag{6}$$

Because the interior temperature will span a wide range of values, the constant property assumption may introduce some error. However, this approximation is tolerable because 1) the properties don't change dramatically over our temperature range (approximately 10%), 2) extreme temperatures are only seen in a very small location and for short times, so the impact is reduced, and 3) other approximations in the comparison to real gun data limit our accuracy anyway.

In the present problem, the boundary function is arbitrary and unknown. Duhamel's theorem can be used with a piecewise constant approximation to the heat flux to generate a general solution. The temperature can be written as a superposition of solutions for heat flux at each time step as

$$\theta_i(x) = \sum_{j=0}^{i} \frac{2}{kL}(q_j - q_{j-i}) \sum_{m=1}^{\infty} \frac{\cos(\beta_m x)}{\beta_m^2} \exp(-\alpha\beta_m^2 (i-j)\Delta t), \tag{7}$$

where the heat flux at $t \leq 0$ is zero and Δt is the time step between measurement samples. Therefore the time when the temperature is calculated corresponds to the time when the measurements are taken. In general, the time step does not have to be constant, but the foregoing analysis does not require this added complexity. Realize that this time is somewhat ambiguous because to obtain a single measurement requires a pulse to be induced, traverse the medium and be detected by the sensor. However, during this traversal, we assume that the thermal transients are negligible. As such, the thermal transients must be smaller than the time of flight for the ultrasonic pulse. Based on an acoustic velocity of $5096\,\mathrm{m/s}$ and wall thickness of $0.064\,\mathrm{m}$, the pulse transit time is of the order of $30\,\mu\mathrm{s}$ (see Table 1). The measured temperature rise occurs over $3\,\mathrm{ms}$, which is two orders of magnitude greater, so our assumption is justified.

Acoustical propagation

The system considered here uses ultrasonic pulses to deduce the transit time of acoustic energy across a solid. The round-trip time for an acoustical pulse to traverse a wall is given by

$$G_i = \frac{2}{c_o} \int_0^L \frac{dx}{1 - P\theta_i(x)} \tag{8}$$

where G_i is a function of when the pulse is triggered. c_o is the base acoustic velocity of the material, P is the acoustical correction factor, and θ is the temperature distribution in the wall. This equation is an expression of the travel time based on a sound speed in the material. If the sound speed is constant, then the travel time is

$$G = \frac{2L}{c_o}, \tag{9}$$

where L is the traversal length—the factor of 2 arises because the wave travels through L and then returns before it is detected. If the sound speed is a function of temperature, then we must integrate over the length

$$G = 2\int_0^L \frac{dx}{c(\theta(x))}. \tag{10}$$

The velocity function is approximated as a linear function of temperature with

$$c(\theta(x)) = c_o(1 - P\theta(x)), \tag{11}$$

The relationship in equation 8 must be evaluated numerically because closed-form solutions are not forthcoming.

The acoustical correction factor is determined by measuring the time of flight of an acoustic wave through a known length of the material at a constant temperature. A calibration curve is generated by measuring the time of flight at various steady temperatures. The slope of the curve is P. In general P doe snot have to be linear in temperature. However, in the present case, the plot is linear over a wide range of temperatures, therefore P is treated as a constant.

Inverse method

By comparing the measured travel time, G, to a calculated travel time, $\hat{G}$, and minimizing the objective

$$S = (G - \hat{G})^T (G - \hat{G}) \tag{12}$$

an estimate of the unknown boundary can be obtained. This is accomplished by guessing a value for the heat flux at a time step, using that value to obtain $\hat{G}$, and evaluating equation 12. The iterated solution is linearized with the sensitivity

$$\frac{dG}{dq} = \frac{G(\hat{q} + \delta q) - G}{\delta q}. \tag{13}$$

The expression for sensitivity is normalized as

$$X^* = \left(\frac{dG}{dq}\right)^* = \left(\frac{dG}{dq}\right)\left(\frac{q_{max}}{G_{base}}\right), \tag{14}$$

where q_{max} is the maximum estimated heat flux value, and G_{base} is the time of flight for an acoustical pulse when the system is at constant, ambient temperature. To maintain stability and speed up convergence, the heat flux estimate for the previous time step is used as an initial guess for the current time step.

A naïve solution approach matches the data exactly at each time step [11]. To reduce the amplification of measurement noise, a function specification approach is used. This approach relaxes the exact matching of the data and fits a presumed functional form of the unknown heat flux to the measured data. In this way a bias based on future behavior is introduced, and the stability of the solution is improved. Excessive bias can degrade the estimate, so careful studies of the effects of the number of future times must be performed.

RESULTS

Verification examples

In order to validate the method, data were generated from three assumed heat flux profiles. These heat flux input functions all contained the same amount of energy ($3.75 \times 10^6\,\mathrm{J/m^2}$) and persist over the same time interval. These assumed heat fluxes mimic the experimental conditions to be considered later. The forward solution was used to generate corresponding temperature response in the wall. These data were integrated to obtain a time of flight for an ultrasonic pulse. These times of flight were then used as calibration data for evaluating the proposed solution approach.

Figure 2 shows the idealized cases of heat flux used to evaluate the solution method. Case 1 is a square wave, with a period of 0.06 s and amplitude of $6.25 \times 10^7\,\mathrm{W/m^2}$. Case 2 is a triangular wave, with a period of 0.06 s and a maximum amplitude of $1.25 \times 10^8\,\mathrm{W/m^2}$. Case 3 is a reverse saw-tooth wave with a period of 0.06 s and the same amplitude as Case 2. The resulting temperatures at the interior surface are also shown in Figure 2 along with the time of flight data for each case, generated for the validation.

Gaussian, zero-mean noise was added to the calibration data to simulate the actual noise level in the ultrasonic measurement data discussed in the experimental results section. The noise level extracted from actual measurements during steady state was approximately 0.5%. This value is small because of the maturity of acoustic measurement capabilities. This low noise level will be crucial in the ability to accurately characterize the heating using ultrasonic pulses. The simulated data with noise are shown in Figure 3. These data illustrate how the time of flight is a function of the total amount of energy in the system and not necessarily of the temperature distribution. After the heat has been added, the time of flight remains relatively constant, even though a steep gradient exists in the wall. Equation 8 shows how the time of flight is an integral over the entire temperature distribution, so this feature is not unexpected.

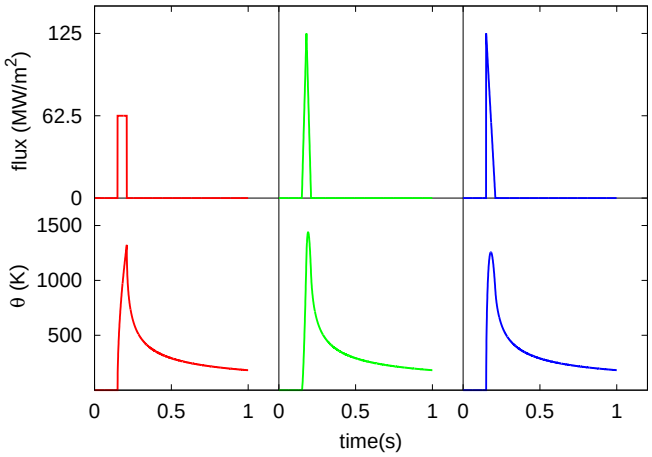

Figure 2. Calibration heat flux data. Case 1 is a square wave, Case 2 is a triangular wave, and Case 3 is a reverse saw-tooth wave. Data shown are heat flux in the first row, with associated internal temperature and acoustic pulse time of flight respectively in following rows.

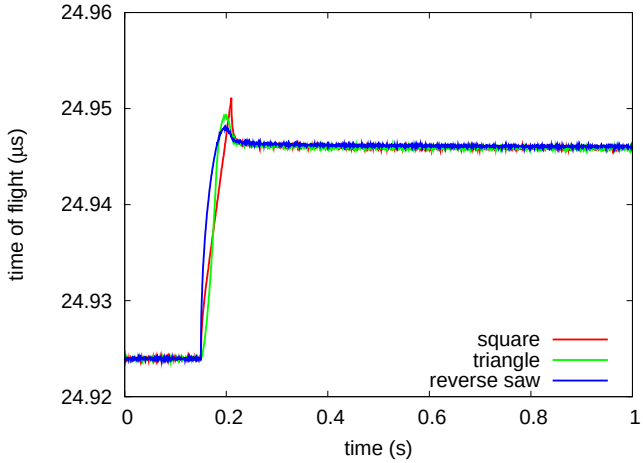

Figure 3. Pulse time of flight calibration data with representative noise added.

Heat flux estimates were obtained using exact matching and a function specification method assuming a piecewise constant heat flux using $1-6$ future time steps to evaluate the appropriate amount of bias for this particular solution.

The heat flux estimates shown in Figure 4 are the result of applying the solution method to the noisy time-of-flight data for Case 3, the reverse saw-tooth wave. Note the extremely low noise level in the measurements of the time of flight of the acoustical pulse. Figure 4 also shows the reconstructed temperature of the internal surface of the system. This figure shows the results

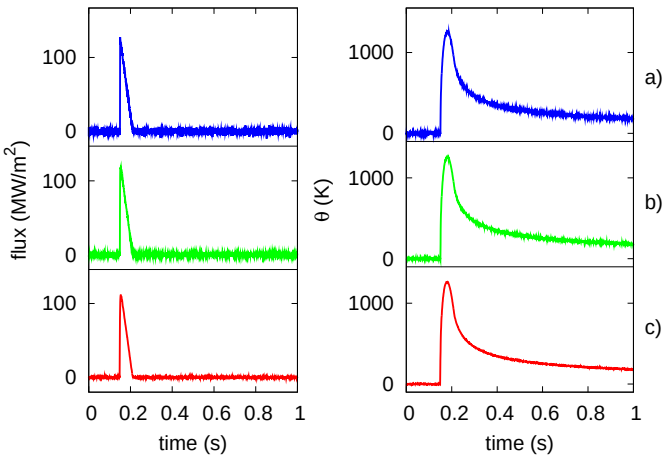

Figure 4. Heat flux and temperature estimate comparison. a) exact matching b) 1 future time c) 4 future times.

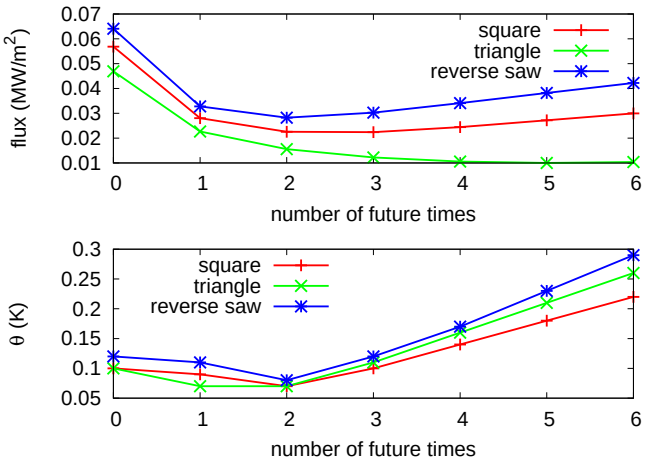

Figure 5. Heat flux and temperature estimation RMS errors for individual solution methods. Straight line segments between data points have been added to guide the eye.

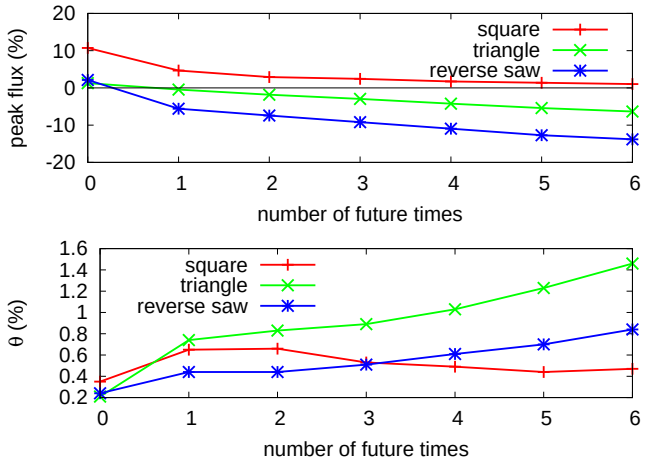

Figure 6. Peak heat flux and peak temperature estimation errors for individual solution methods. Negative errors indicate underestimation of parameters with respect to quantities; positive errors indicate overestimation. Straight line segments between data points have been added to guide the eye.

of the analysis using exact matching along with 1 and 4 future times.

Instabilities in inverse solutions always show up where gradients are large. In the Case 3, the heat flux rises instantaneously, which normally results in over-estimation of the boundary flux and represents the worst-case scenario for an estimation procedure to handle. The future times introduce bias and have limited the ability to capture the precise peak. Figures 5 and 6 show the errors in the estimates of the peak values of both the heat flux and the maximum temperature of the internal surface of the system for each case using the proposed solution method. Note that the errors associated with estimated heat flux are larger than the ones associated with the estimation of peak temperature. This is due to the ill-posed nature of the problem, in that the solution for temperature from a boundary heat flux can generally be expressed as a Volterra equation of the second kind. Errors of the solution are therefore unbounded [12], resulting in amplification of the measurement noise. The values shown in Figures 5 and 6 reflect the observation that little bias is required to obtain an acceptable solution due to the extremely low noise level in the measured quantity.

The rms errors shown in Figure 5 were calculated with

$$\varepsilon_{rms} = \frac{\sqrt{\sum_{p=1}^{N}(\psi_{actual} - \psi_{est})^2}}{N}, \qquad (15)$$

where N is the number of data points, and ψ is the quantity of interest, here either heat flux or temperature. The peak errors were calculated with

$$\frac{\psi_{est} - \psi_{actual}}{\psi_{actual}} \times 100\%, \qquad (16)$$

such that a positive error indicates an overestimation of a quantity and a negative error indicates underestimation.

The sensitivity of the measured quantity to changes in estimated heat flux was calculated to determine confidence intervals for the estimates. A test heat flux case consisting of a single time step of non-zero heat flux was input into the system, and the resultant change in pulse transit time associated with this change in flux was quantified. Since the measured quantity in

Table 1. Material properties of Navy gun barrel used to predict heating from ultrasonic measurements.

Property	**value**
Material Density (ρ)	$7833\,\mathrm{kg/m^3}$
Thermal Conductivity (k)	$44.5\,\mathrm{W/mK}$
Specific Heat Capacity (C_p)	$475\,\mathrm{J/kgK}$
Base Acoustic Velocity (c)	$5095.5\,\mathrm{m/s}$
Acoustic Velocity Coefficient (P)	$55\times10^{-6}\,\mathrm{K^{-1}}$
Wall Thickness (L)	$0.0635\,\mathrm{m}$

this case involves an integration over the temperature distribution, the character of this sensitivity is very different than sensitivities of normal IHCPs. The quantity G is related more to the amount of energy in the system and not the magnitude of the temperature. In the case of a single pulse of energy, the amount of energy in the system is constant until the energy has diffused across the domain, which is much longer than the experimental time considered in this example. Because the amount of energy in the system is relatively constant in time, G does not change in time either. As a result, the sensitivity is constant in time after the pulse. For this analysis the change in G after the pulse ($2.312\times10^{9}\,\mathrm{s}$) is used in equation 13, along with the heat flux required to manifest the change ($1\times10^{8}\,\mathrm{W/m^2}$). This ratio is normalized as indicated in equation 14. The resulting normalized sensitivity was 9.227×10^{-5}. This normalized sensitivity is much smaller than is usually considered useable for most inverse heat conduction problems. However, because the measurement noise is so small, accurate solution are still possible. In fact, the 95% confidence interval on the estimates is approximately $\pm5\%$ of the actual value.

Experimental example

The estimation method was applied to data collected at the Naval Surface Warfare Center in Dhalgren Virginia. The data were gathered during the firing of a Mark 45 Naval Gun. The physical constants for the problem were based on the gun being constructed with AISI 4340 (UNS G43400) steel.

Figure 7 shows the raw transit time data. The abrupt drop in the transit time has been attributed to a non-related physical phenomenon of the firing of the gun system and is not related to the thermal effects on acoustic velocity. This effect produces non-real cooling and temperature decreases in the calculated data and is neglected in the context of this work.

Figure 8 shows the calculated temperature history of the interior of the gun barrel. These data are calculated, along with the heat flux shown in Figure 9 using 2 future time steps to reduce the

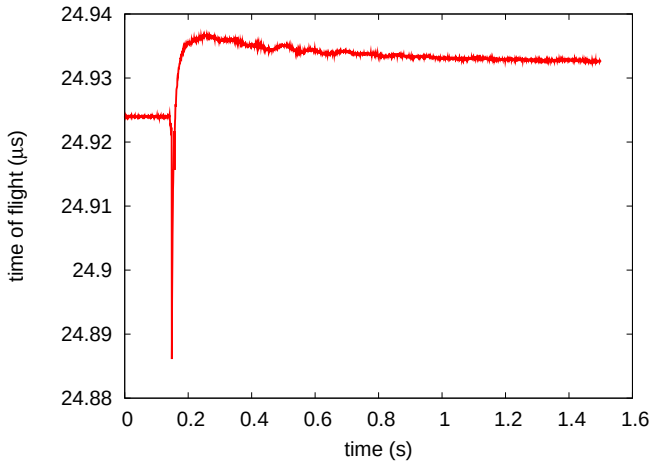

Figure 7. Experimental data, time of flight of an acoustic pulse.

noise in the result. The selection of 2 future times deserves some justification. In the present case, we are interested in the shape of the pulse more than the magnitude at the peak because we are trying to identify events within the barrel over time, not the maximum temperature reached, which is difficult to verify. Therefore, by adding bias (2 future times), we obtain a more faithful overall representation for the heat flux as suggested by the analysis in Figure 5. Additional bias does not improve the estimates significantly. If we were interested in the peak value, then the analysis in Figure 6 suggests that fewer (possibly 0) future times are required. Furthermore, ability to capture the peak temperature through adjusting the number of future times is strongly dependent on the type of heating that occurs. Therefore, we are willing to sacrifice the peak values in favor of low RMS errors, which can reliably be obtained.

Based on the analysis of the calibration data, it is estimated that the maximum heat flux is underestimated by no more than 6%, which is the percentage of the reverse sawtooth for 3 future times, and that the actual peak temperature is 4°C lower than shown based on 0.5% temperature error from the sawtooth at 2 future times. Realize that the 5.6% error from test Case 3 was a worst case. Because the actual heat flux does not rise instantaneously, a better matching of the peak heat flux is likely obtained.

The curve shown in Figure 9 is indicative of a short duration, high temperature event inside the gun barrel. The oscillations in the temperature data starting at about seconds is more difficult to explain, perhaps attributable to effects of flow of combustion products out of the barrel after firing, and the associated equalization of pressure with the ambient level. These oscillations could also be due to changes in the barrel dimensions attributable to the vibration of the system as a result of the firing event. In any case this effect can also be seen in the time of flight data shown in Figure 7. The maximum temperature indicated by the calculated

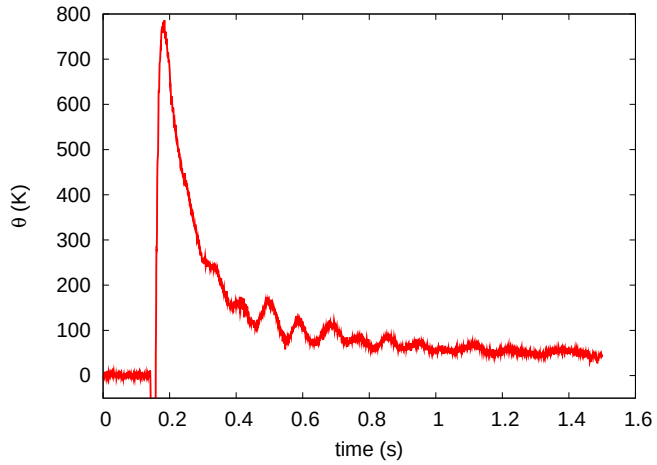

Figure 8. Temperature of internal surface of the gun barrel.

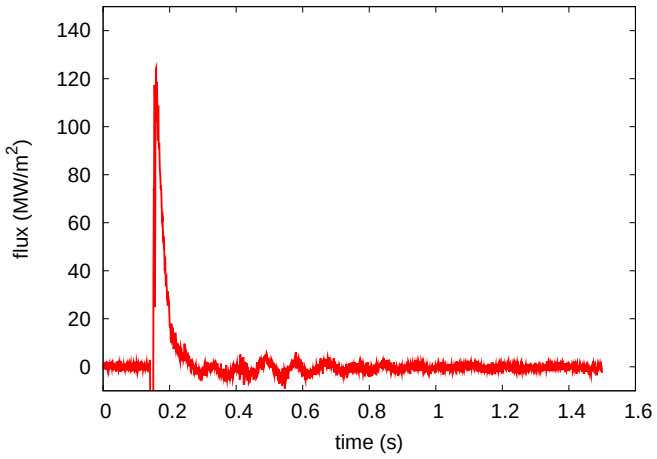

Figure 9. Heat flux at gun bore interface.

data of 789.4°C is in approximate agreement with the maximum estimated bore temperature of 944°C. This quantity is estimated with [13]

$$T_{max} = \frac{T_f - 540}{1.8 + 7130 d^{2.22} m_c^{-0.86} v_m^{-0.86}} + 300, \qquad (17)$$

where T_f is propellant flame temperature, d is bore diameter, m_c is the mass of the propellant charge and v_m is the projectile muzzle velocity. For the case presented here the data are given in Table 2.

The maximum heat flux indicated by the data of $120\,\mathrm{MW/m^2}$ is reasonable based on predictions of the amount of total propellant charge energy lost as heat when firing a projectile. Knowing the mass of the projectile to be 31 kg, the kinetic energy of the projectile is calculated to be 10.7 MJ. A 7 kg charge contains about 33.1 MJ of energy. Therefore, the gun efficiency is approximately 33%, which is typical [14]. Heat loss to the barrel is estimated at 66.9% of the total energy of the propellant, or about 22.1 MJ. The integral of Figure 9 can be approximated as the area in a triangle—$0.5 \times 120\,\mathrm{MW/m^2} \times 0.1\,\mathrm{s} \times = 6\,\mathrm{MJ/m^2}$. If the area of the barrel is $3.83\,\mathrm{m^2}$ then the energy is 22.98 MJ, which is less than 4% off from the estimates. Of course some of the enthalpy in the propellant is blown out the end, and the energy deposited is not done so uniformly. Nevertheless, the approximation appears to agree well with the estimates from time of flight data.

Table 2. Gun parameters used to determine heat flux resulting from friction between projectile and barrel during firing.

parameter	value
v_m	$831\,\mathrm{m/s}$
d	$0.155\,\mathrm{m}$
m_c	$8.3\,\mathrm{kg}$

CONCLUSIONS

A method for remotely determining temperature and heat flux on an interior surface has been presented. The class of problems is new in terms of inverse heat conduction problems because the residual of ultrasonic time of flight data is minimized—not temperature. Nevertheless, a standard inverse technique was used to estimate the internal boundary condition on data gathered in a field test of a naval gun. Estimates are in good agreement with published predictions, and test cases suggest that estimates of peak heat flux could be off by as little as 5%. Additional effort needs to be devoted to examining different time stepping schemes, sample rates and different geometries and material properties on the sensitivity of the estimates to assess the utility of using ultrasonic temperature measurements for remote heat flux determination. The preliminary evidence for the efficacy using ultrasonic pulse measurements to remotely and non-intrusively measure a boundary heat flux is extremely encouraging.

ACKNOWLEDGMENTS

This work was supported in part by AFOSR (contract # FA9550-06-C-0071)

REFERENCES

[1] Yee, B. G. W., and Couchman, J. C., 1976. "Application of ultrasound to NDE of materials". *IEEE Transactions on Sonics and Ultrasonics*, **SU-23**(5), Sept., pp. 299–305.

[2] Hoyle, B. S., and Luke, S. P., 1994. "Ultrasound in the process industries". *Engineering Science and Education Journal*, **3**(3), pp. 119–122.

[3] Green, S. F., 1985. "An acoustic technique for rapid temperature distribution measurements". *Journal of the Acoustical Society of America*, **77**(2), Feb., pp. 759–763.

[4] Fife, S., Andereck, C. D., and Rahal, S., 2003. "Ultrasound thermometry in transparent and opaque fluids". *Experiments in Fluids*, **35**, pp. 152–158.

[5] Chen, G., 1999. "Phonon wave heat conduction in thin films and superlattices". *Journal of Heat Transfer*, **121**, Nov., pp. 945–953.

[6] Baharis, C., and Cornish, R., 1991. "Ultrasonic detection of heat fronts in continuously cast steelproduct". In Proceedings of the Ultrasonics Symposium, Vol. 2, pp. 957–960.

[7] Wadley, H. N. G., Norton, S. J., Mauer, F., Droney, B., Ash, E. A., and Sayers, C. M., 1986. "Ultrasonic measurement of internal temperature distribution". *Philosophical Transactions of the Royal Society of London. Series A, Mathematical and Physical Sciences*, **320**(1554), Nov., pp. 341–361.

[8] Berryman, J. G., 1990. "Stable iterative reconstruction algorithm for nonlinear traveltime tomography". *Inverse Problems*, **6**(1), pp. 21–42.

[9] Beck, J. V., Blackwell, B., and St. Claire Jr., C. R., 1985. *Inverse Heat Conduction: Ill-Posed Problems*. Wiley-Interscience.

[10] Özişik, M. N., 1968. *Boundary Problems of Heat Conduction*. Dover Publications, Inc., New York.

[11] Stolz, Jr., G., 1960. "Numerical solutions to an inverse problem of heat conduction for simple shapes". *Journal of Heat Transfer*, **82**, pp. 20–26.

[12] Kress, R., 1989. *Linear Integral Equations*, Vol. 82 of *Applied Mathematical Sciences*. Springer-Verlag.

[13] Johnston, I. A., 2005. Understanding and predicting gun barrel erosion. Tech. Rep. DTSO-TR-1757, Australian Government Department of Defense, Aug.

[14] Corner, J., 1950. *Theory of the Interior Ballistics of Guns*. John Wiley & Sons, Inc., New York.